RADIATIVE FORCING OF URBAN AEROSOLS IN THE VISIBLE REGION

B. I. Tijjani
Department of Physics, Bayero University, Kano.
Emails: idrith@yahoo.com, idrithtijjani@gmail.com.

ABSTRACT

The optical and microphysical properties of urban aerosols at the visible region (0.40μm to 0.75μm) at relative humidities (RHs) 0, 50, 70, 80, 90, 95, 98 and 99% are extracted from the Optical Properties of Aerosol and Clouds software. The optical parameters extracted are refractive indices, radii of water soluble components, scattering, absorption, and extinction coefficients, single scattering albedos, asymmetry paramenters and τ_{sca} and τ_{aba} as the aerosol layer scattering and absorption optical thickness. The data was used to calculate the radiative forcings(RF), Angstom parameters, hygroscopic growth factors, and hgroscopicities. Angstrom parameters that are used to determine the nature of the particles size distributions at different RHs are obtained using the aerosols optical depths. Angstrom parameters increase from 1.0842 at 0% RH to 1.1677 at 80% RH as a result of hygroscopic growth and decrease from 1.1677 at 80% RH to 0.9722 at 99% as a result of coagulation due to the increase in RH. It also shows that increase in RH has caused increase in mode size distributions which caused increase in radiative cooling. The analysis further shows that these aerosols have Junge type of size distributions and are dominated by fine mode particles distribution which account for the observed negative RF.

INTRODUCTION

Anthropogenic aerosols affect the Earth's climate in two ways: they reflect and absorb solar radiation, thereby giving rise to what is referred to as the direct radiative forcing, and they increase the numbers and decrease the sizes of cloud droplets, thereby giving rise to the indirect radiative forcing [1-3]. Both effects alter sunlight reflected and absorbed by the Earth-

atmosphere system. These changes are expected to lead to changes in atmospheric and oceanic temperatures, and consequently, altered weather patterns. Knowledge of the spatial distribution of aerosols and their effect on the Earth's energy budget is a key to reliable assessments of climate change. The variability of aerosol concentrations coupled with the variability of their physical and optical properties, makes direct measurements of aerosols and their properties on global scales impractical. Consequently, remote sensing of aerosols from satellites is essential to determining the temporal and spatial distribution of aerosols and estimating the aerosol direct radiative forcing of climate.[4].

Radiative forcing due to aerosols is one of the largest sources of uncertainties in estimating anthropogenic climate perturbations [1, 5]. Aerosols are produced by various sources that are highly inhomogeneous in both time and space [6-10], as a result of which estimating aerosol radiative forcing is much more complicated than estimating radiative forcing due to well-mixed greenhouse gases [5]. The data on aerosol physical and optical characteristics (such as aerosol optical depth and size distribution) are more readily available than data on aerosol chemical composition. This is because the determination of chemical composition requires dedicated field experiments and expensive instrumentation [11]. One of the important properties of aerosols is the Aerosol Optical Depth (AOD). Measuring AOD at different spectral wavelengths helps in deriving information on the optical properties and size distribution of particles, as well as studying the diurnal and season variability of aerosols [12].

The absorption of water by atmospheric aerosols with increasing relative humidity (RH) influences their size, composition, lifetime, chemical reactivity, light scattering and other optical and microphysical characteristics. Water is the most prevalent aerosol component at RHs above 80% and is often a significant component at lower RHs [13]. Accordingly, hygroscopic growth is

important in a number of air pollution problems, including visibility impairment, climate effects of aerosols, acid deposition, long-range transport, and the ability of particles to penetrate into the human respiratory system.

The aim of this paper is to calculate and analyze the spectral behavior of RF of Urban aerosols in the visible region and the effect of hygroscopic properties of the ambient aerosols on it. Also the spectral behavior of other optical parameters analysed are, optical depths, Angstrom parameters, single scattering albedos, asymmetry parameters, and extinction, scattering and absorption coefficients to help in determining the nature of the aerosols such as well as the size distribution..

METHODOLOGY

The data used for the urban aerosols in this paper are derived from the Optical Properties of Aerosols and Clouds (OPAC) data set [14]. In this, a mixture of three components is used to describe Urban aerosols: a water soluble components (WASO, consists of scattering aerosols, that are hygroscopic in nature, such as sulfates and nitrates present in anthropogenic pollution), water insoluble (INSO) and soot (SOOT, not soluble in water and therefore the particles are assumed not to grow with increasing relative humidity).

[15] derived the formula that can be used to calculate the globally averaged direct aerosol Radiative forcing of absorbing aerosols, ΔF_R, as

$$\Delta F_R = -\frac{S_0}{4} T_{atm}^2 (1-N)\{(1-A)^2 2\beta\tau_{sca} - 4A\tau_{abs}\} \quad (1)$$

Where S_0 =1370Wm^{-2} is a solar constant, T_{atm} =0.79 is the transmittance of the atmosphere above the aerosol layer, N =0.6 is the fraction of the sky covered by clouds, the global averaged albedo A=0.22 over land, β is the fraction of radiation scattered by aerosol into the atmosphere and τ_{sca} and τ_{aba} are the aerosol layer scattering and absorption optical thickness [16]. The above

expression gives the radiative forcing due to the change of reflectance of the earth-aerosol system. The upscattering fraction is calculated using an approximate relation [17]

$$\beta = \frac{(1-{}^{g}/_{2})}{2} \quad (2)$$

where g is the asymmetry parameter.

To calculate the effective refractive indices of the bulk samples the following formula is used for the three mixed aerosols [18]:

$$\frac{\varepsilon_{eff}-\varepsilon_0}{\varepsilon_{eff}+2\varepsilon_0} = \sum_{i=1}^{3} f_i \frac{\varepsilon_i-\varepsilon_0}{\varepsilon_i+2\varepsilon_0} \quad (3)$$

Where f_i and ε_i are the volume fraction and dielectric constant of the i^{th} component and ε_0 is the dielectric constant of the host material. For the case of Lorentz-Lorentz [19, 20], the host material is taken to be vacuum, ε_0 =1.

The spectral behavior of the aerosols optical depth (τ) (or scattering (σ_{scat}), absorption (σ_{abs}) and extinction (σ_{ext}) coefficients) can be used to obtain some information regarding the size distribution by just looking at the Angstron coefficient exponent that expresses the spectral dependence of any of the optical parameters with the wavelength of light (λ) as inverse power law [21,22]:

$$\tau(\lambda)=\beta\,\lambda^{-\alpha} \quad (4)$$

The wavelength dependence of $\tau(\lambda)$ can be characterized by the Angstron parameter, which is a coefficient of the following regression:

$$\ln\tau(\lambda) = -\alpha\ln(\lambda) + \ln\beta \quad (5)$$

where β and α are the turbidity coefficient and the shaping factor, respectively.[23, 24] α is also related to the size of particles. So α and β can be used to describe the size distribution of aerosol particles and the general haziness of the atmosphere respectively. Larger particles generally correspond to smaller α, whereas smaller particles generally correspond to larger α. According to [25] a low (down to 0) is a sign of large dust particles; a high (up to 2) corresponds to small smoke particles. According to [26] typical values of the shaping factor are larger than 2.0 for fresh smoke particles. The dust studies seem to yield shaping factors in the range of approximately 0.2, whereas particles produced from biomass burnings yielded shaping factors around 1.5 and higher. The formula is derived on the premise that the extinction of solar radiation by aerosols is a continuous function of wavelength, without selective bands or lines for scattering or absorption [27].

As a result of wetting the hydroscopic particles grow, thereby changing the effective radius of an aerosol mixture and subsequently the aerosol extinction or aerosol optical thickness. The variation of the extinction coefficient or the aerosol optical thickness with the wavelength can be presented as a power law function with a constant (related to the power factor) known as the Ångström coefficient [22]. When the particle size distribution is dominated by small particles, a situation usually associated with pollution, the Ångström coefficients are high; in clear conditions they are usually low. [28] demonstrated that the Ångström coefficient can be used as a tracer of continental aerosols. With changing atmospheric conditions and rising or falling RH, the measured aerosol optical thickness/extinction likewise changes, and so does the Ångström coefficient.

To quantify the water uptake at subsaturated conditions, we define the hygroscopic growth factor (HGF) as the ratio of the radius R_{RH}, at a specified RH to the original dry diameter R_{dry}, which is

at RH =0% and RH is taken for seven values 50%, 70%, 80%, 90%, 95%, 98% and 99%. [29, 30]:

$$HGF = \frac{R_{RH}}{R_{dry}} \quad (6)$$

The HGF can be subdivided into different classes with respect hygroscopicity. One classification is based on diameter growth factor by [23, 29] as Barely Hygroscopic (HGF = 1.0–1.11), Less Hygroscopic (HGF = 1.11–1.33), More Hygroscopic (HGF = 1.33–1.85) and most hygroscopic growth (HGF > 1.85).

The hygroscopic growth of aerosols influences the particle size distribution and refractive indices and hence, several key optical properties of aerosols (e.g., scattering, extinction and absorption coefficients, single scattering albedo, asymmetry parameter, and aerosol optical depth) that are relevant to aerosol radiative forcing estimates [31-33].

The aerosol hygroscopic growth factor, f(RH,λ), describes the ratio of aerosol light extinction between two different RH values that can be calculated from the following [34]:

$$f(RH,\lambda) = \frac{\sigma_{ext}(RH_{high})}{\sigma_{ext}(RH_{ref})} = \left(\frac{100-RH_{ref}}{100-RH_{high}}\right)^{\gamma} \quad (7)$$

where in our study RH_{ref} = 00%. The γ parameter in our case was obtained by combining the eight $\sigma_{ext}(\lambda)$ measurements at 00%, 50%, 70%, 80%, 90%, 95%, 98% and 99% RH. The use of γ has the advantage of describing the hygroscopic behavior of aerosols in a linear manner over a broad range of RH values; it also implies that particles are deliquesced [35], a reasonable assumption for this data set due to the high ambient relative humidity during the field study. The γ parameter is dimensionless, and it increases with increasing particle water uptake. From previous studies, typical values of γ for ambient aerosol ranged between 0.1 and 1.5 [35-37].

RESULTS AND DISCUSSIONS

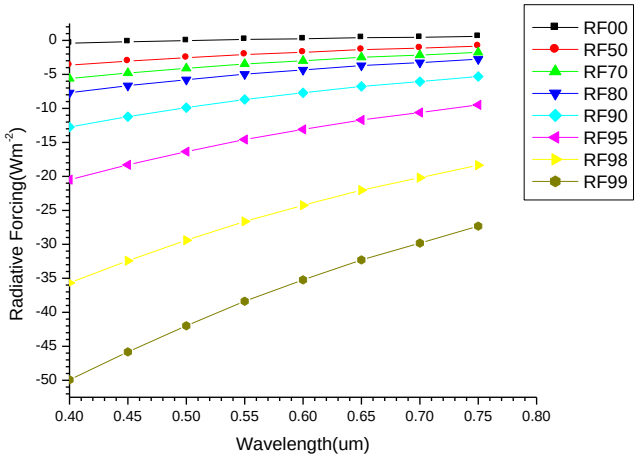

Figure 1: Radiative forcing against wavelength

It shows smooth decrease in radiative cooling with wavelength but increases with the increase in RH. The relation of RF with RH is such that at the deliquescence point (90 to 99%) this growth with higher humidities increases substantially, making this process strongly nonlinear with relative humidity. The reason why radiative cooling is higher in the lower wavelengths with the increase in RHs is because as a result of hygroscopic growth, smaller particles scatter more light than bigger particles; this implies more cooling at lower wavelength with hygroscopic growth. Therefore this shows that the hygroscopicity of atmospheric aerosols greatly affect their ability to scatter more light than absorbed.

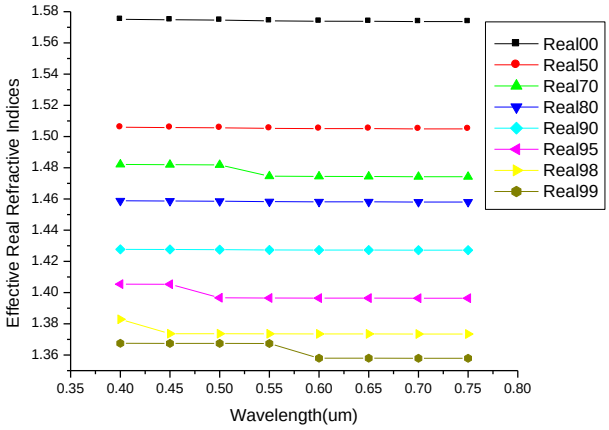

Figure 2: A plot of effective real refractive indicies against wavelength.

The figure shows that refractive indicies decreases with the increase in RH, but constant with wavelength at the point where the particles are assumed spherical and variable where the particles are non-spherical (at 70, 95, 98 and 99%) as pointed out by [38]. These variations may also be due to variations in the mixing state of different components of the aerosols due to changes in RH.

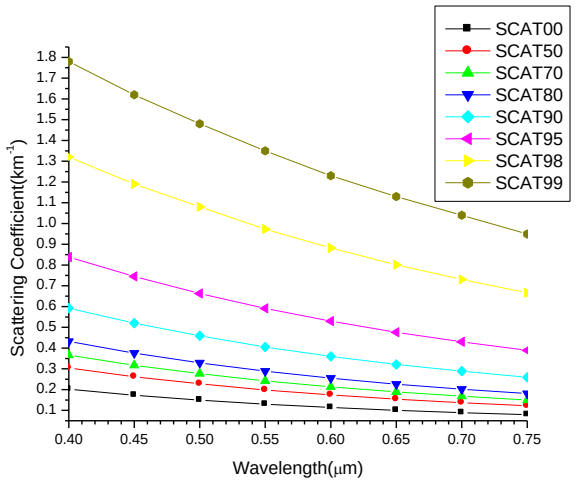

Figure 3: A graph of scattering coefficients against wavelength.

The scattering coefficient follows a relatively smooth decrease with wavelength for all RHs and can be approximated with power law wavelength dependence (Scattering Angstrom Exponent). It is evident from the figure that there is relatively strong wavelength dependence of scattering coefficients at shorter wavelengths that gradually decreases towards longer wavelengths irrespective of the RH, attributing to the presence of fine and coarse particles. The presence of a higher concentration of the fine-mode particles which are selective scatters enhances the irradiance scattering in shorter wavelength only while the coarse-mode particles provide similar contributions to the scattering coefficients at both wavelengths [39]. It also shows that as a result of hygroscopic growth, smaller particles scatter more light at shorter wavelengths compared to bigger particles. The relation of scattering coefficients with RH is such that at the deliquescence point (90 to 99%) this growth with higher humidities increases substantially, making this process strongly nonlinear with relative humidity [40-43].

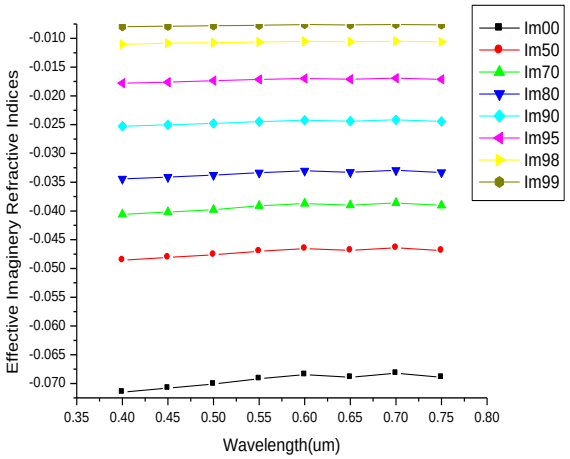

Figure 4: A plot of effective imaginary refractive indices against wavelength.

It shows a slight increase with the increase in wavelength but decrease in magnitude with RH. This shows that as a result of hygroscopic growth, there is a decrease in effective imaginary

refractive indices.

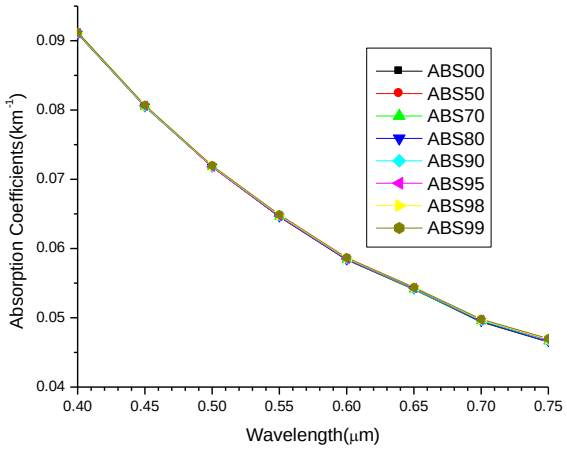

Figure 5: A plot of absorption coefficients against wavelengths

It shows that absorption coefficients decrease smoothly with wavelength but constant in all RHs and can be approximated with power law wavelength dependence (Absorption Angstrom Exponent). It also shows hygroscopic growth has no effect on absorption coefficients.

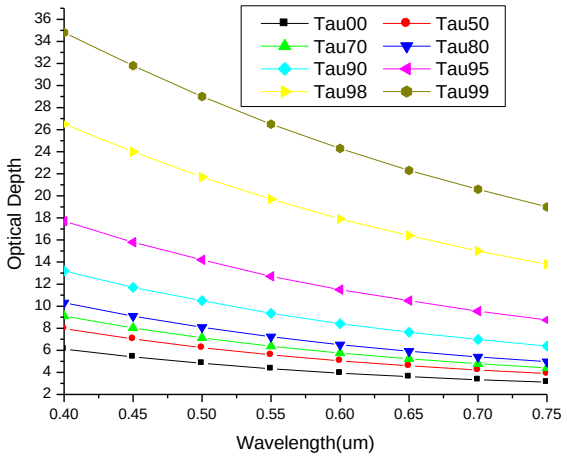

Figure 6: A plot of optical depth against wavelength

The optical depth follows a relatively smooth decrease with wavelength for all RHs and can be approximated with power law wavelength dependence (Optical Depth Angstrom Exponent). It is evident from the figure that there is relatively strong wavelength dependence of optical depth at shorter wavelengths that gradually decreases towards longer wavelengths irrespective of the RH, attributing to the presence of fine and coarse particles. The presence of a higher concentration of the fine-mode particles which are selective scatters enhances the irradiance scattering in shorter wavelength only, while the coarse-mode particles provide similar contributions to the AOD at both wavelengths [39]. The relation with RH shows that hygroscopic growth has more effect on fine particles than coarse particles and also that has caused increase in mode size distributions. The relation of optical depth with RH is such that at the deliquescence point (90 to 99%) this growth with higher humidities increases substantially, making this process strongly nonlinear with relative humidity [40, 41].The figure shows confirms the power law, and this ascertain equations (4) and (5). A higher RH could obviously cause the particles' hygroscopic increase, which could result in greater extinction and a larger volume of fine particles.

Table 1: Values of α and β obtained from regression analysis using equation(5)

RH(%)	00	50	70	80	90	95	98	99
α	1.0842	1.1458	1.1618	1.1677	1.1613	1.1267	1.0435	0.9722
β	2.2663	2.8075	3.1680	3.5732	4.6263	6.4183	10.4136	14.6078
R^2	0.9999	0.9998	0.9996	0.9993	0.9987	0.9979	0.9965	0.9954

The observed variations in Ångström coefficients can be explained by changes in the effective radii of the mixtures resulting from changes in RH in the range 0% to 80%: the larger the number of small aerosol particles, the smaller the effective radius and the larger the Ångström coefficient The Ångström exponent increases with the increase in water vapor, which means that the effective radius of the aerosol particles become smaller when the water vapor increases.. But as from 80% to 99% RH there is an increase in fine mode particle radius which results from particle

growth due to coagulation and hygroscopic growth. Coagulation rates increase as particle concentration increases [44]; therefore this particle growth mechanism will be greatest at the highest optical depth ($\tau(\lambda)$). Hygroscopic at high RH will also tend to increase optical depth as accumulation mode particles increase in size [26]. Also these values of α in the range 1.1 to 1.2 imply that aerosol mixtures are dominated by fine mode particles and also reflect the occurrence of large size accumulation mode particles that may result from fine particle coagulation at high concentration from hygroscopic growth. The high AOD is linked to a hygroscopic and/or coagulation growth from the fine aerosols. Furthermore, the fine mode aerosols have hydrate and coagulated characters that become large particles, causing the AOD to increase and α becomes smaller. Also the decrease in α as AOD increases, suggest the presence of larger particles leads to enhanced extinction. An increase in AOD with an increasing α as a result of change in RH, reflects the presence of a significant fraction of fine particles in the aerosol size distribution. There is observational evidence that Ångström exponents decrease in value as particles grow hygroscopically [45].

Table 2: Values of dry and wet radii of aerosols extracted from the microphysical characteristics of the aerosols and the calculated HGF using equation(6).

RH(%)	00	50	70	80	90	95	98	99
Rmod (wet), [um]:	0.0212	0.0262	0.0285	0.0306	0.0348	0.0399	0.0476	0.0534
Rmod (dry), [um]:	0.0212	0.0212	0.0212	0.0212	0.0212	0.0212	0.0212	0.0212
HGF	1	1.236	1.344	1.443	1.642	1.882	2.245	2.519
MAS.MIXof WASO(%)	46.41	56.32	60.85	64.75	71.52	78.22	85.35	88.98

Table 2 shows that the mixture is very hygroscopic.

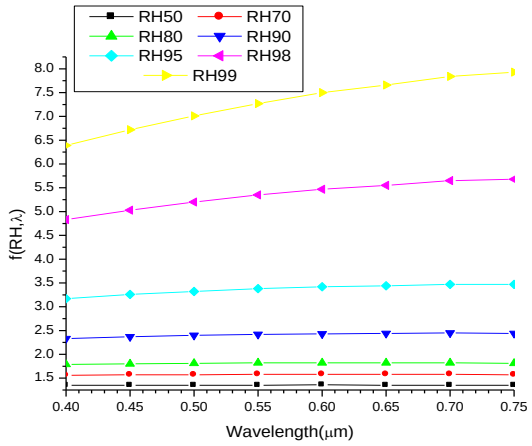

Figure 7: A plot of f(RH, λ) against wavelength

It shows that the f(RH, λ) increases with the increase in RH. But in relation to wavelengths, from 50 to 80%RH it is almost constant, but started increasing with wavelength from 90 to 99 (the slopes increase as the RH increases). At the deliquescence point this growth with higher humidities increases substantially, making this process strongly nonlinear with relative humidity [40, 41]. Comparing figure 7 and table 2 it can be concluded that the particles are very hygroscopic.

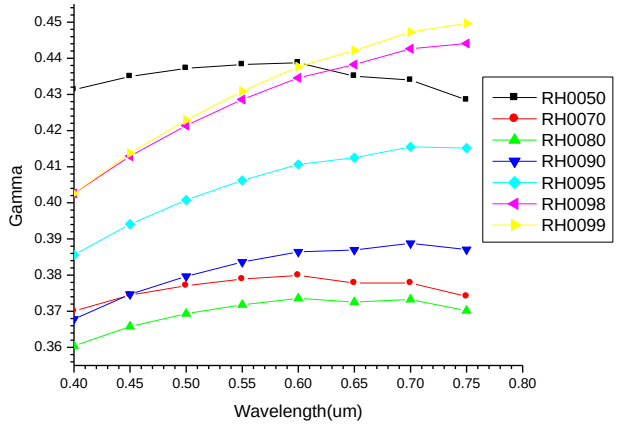

Figure 8: A plot of g against wavelength

These variations may be due to variations in the mixing state of different components of the aerosols due to changes in RH.

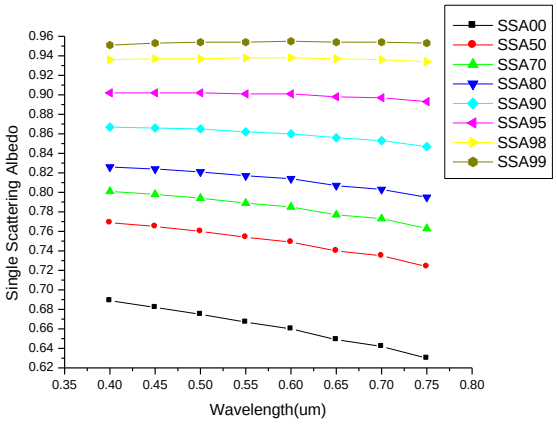

Figure 9: A plot of single scattering albedo against wavelength

It shows that SSA is increasing with increase in RH because as it can be seen on figures 3 and 5, scattering is increasing faster than absorption as a result of hygroscopic growth. The SSA decreases with wavelength because the scattering is decreasing faster than absorption as shown in figures 3 and 5 [38, 46].

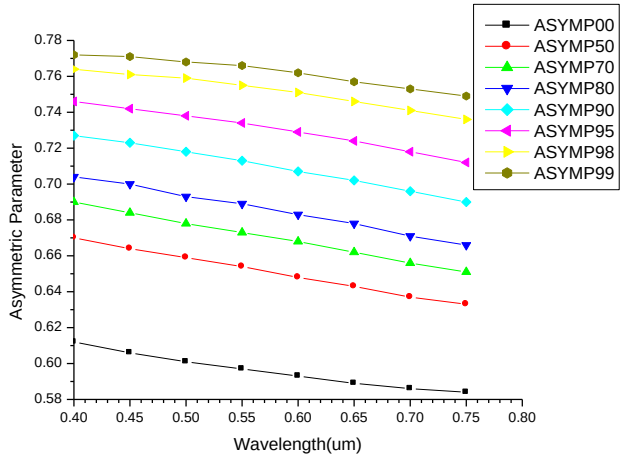

Figure 10: A graph of Assymmetry parameter against wavelengths.

Figure 10 verify that smaller particles scatter more lights than bigger particles as discussed in figure 3 and they scatter more in the forward than backward. It also shows that there is a dominance of fine particles because the asymmetry parameter does not change much with wavelength even as a result of hygroscopic growth. It relation with RH shows that hygroscopic growth enhances scattering in the forward direction.

CONCLUSION

The Radiative Forcing (cooling) at 0% RH linearly decreases to higher wavelength. The negative value of RF at lower wavelength signifies the presence of fine mode particles while the positive values at higher wavelengths signify the presence of coarse mode particles. As the RH is increased it is observed that the RF is more negative at shorter wavelength than higher wavelengths, this signifies the dominance of fine mode particles. Figure 5 shows higher absorption coefficients at shorter wavelengths, which also indicate why cooling results. That is higher absorption results in less radiation reaching the lower atmosphere which induces cooling. Also the value of Angstrom coefficients indicates the dominance of fine particles over coarse particles, and are comparable to those found in pollution outbreaks in the northeast Asian region [47-49]. The observed increase in scattering, which is much more than absorption shows that hygroscopic growth has more effect on fine particles than coarse particles. It can therefore be safely concluded that the dominance of fine particles in this spectral range is what is responsible for the radiative cooling.

REFERENCES

[1] Charlson, R. J., Schwartz S. E., Hales J. M., Cess R. D., Coakley J. A., Hansen J. E., and Hoffmann D. J., (1992): Climateforcing by anthropogenic aerosols. *Science*, **255,** 423–430.

[2] Andreae, M. O., (1995) Climatic effects of changing atmospheric aerosol levels, chap. 10, in World Survey of Climatology, vol. 16, Future Climates of the World, edited by A. Henderson-Sellers, pp. 347– 398, Elsevier Sci., New York,.

[3] Charlson, R. J., and Heintzenberg J. (1995), Dahlem Workshop Report on Aerosol Forcing of Climate, 416 pp., John Wiley, New York,.

[4] Tahnk W. R. and Coakley Jr J. A. (2002), Aerosol optical depth and direct radiative forcing for INDOEXderived from AVHRR: Observations, January–March 1996–2000, JOURNAL OF GEOPHYSICAL RESEARCH, VOL. 107, NO. D19, 8010, 10.1029/2000JD000183,

[5] Houghton, J. T., Meira L. G., Filho, J. P., Bruce, H. Lee, B. A. Callander, and E. F. Haites, (1995) *Climate Change 1994: Radiative Forcing of Climate Change and an Evaluation of the IPCC.* Cambridge University Press, 347 pp.

[6] Shaw, G. E., Regan J. A., and Herman B. M., 1973: Investigations of atmospheric extinction using direct solar radiation measurements made with a multiple wavelength radiometer. *J. Appl. Meteor.,* **12,** 374–380.

[7] Prospero, J. M., et. al., (1983): The atmospheric aerosol system. *Rev. Geophys. Space Phys.,* **21,** 1607–1629.

[8] Bates, T. S., Hubert B. J., Gras J. L., Griffiths F. B., and Durkee P. A., (1998): International Global Atmospheric Chemistry (IGAC) project's First Aerosol Characterisation Experiment (ACE-1): An Overview. *J. Geophys. Res.,* **103,** 16 297–16 318.

[9] Russell, P. B., P. V. Hobbs, and L. L. Stowe, (1999): Aerosol properties and radiative effects in the United States East Coast haze plume: An overview of the Tropospheric Aerosol Radiative Forcing Observational Experiment (TARFOX). *J. Geophys. Res.,* **104,** 2213–2222.

[10] Quinn, P. K., et. al., (2000): A comparison of aerosol chemical and optical properties from the 1st and 2nd Aerosol Characterization Experiments. *Tellus,* **52B,** 239–257.

[11] Satheesh S. K. and Srinivasan J. (2006) A Method to Estimate Aerosol Radiative Forcing from Spectral Optical Depths, JOURNAL OF THE ATMOSPHERIC SCIENCES VOLUME 63, 1082-1092.

[12] Rana S., Kant Y., Dadhwal V. K. (2009), *Diurnal and Seasonal Variation of Spectral Properties of Aerosols over Dehradun, India* Aerosol and Air Quality Research, Vol. 9, No. 1, pp. 32-49, 2009

[13] Hanel, G. (1976). The Properties of Atmospheric Aerosol Particles as Functions of Relative Humidity at Thermodynamic Equilibrium with Surrounding Moist Air. In *Advances in Geophysics, Vol. 19,*H. E. Landsberg and J.Van Mieghem, eds., Academic Press, New York, pp. 73–188.

[14] Hess M., Koepke P., and Schult I (May 1998), Optical Properties of Aerosols and Clouds: The Software Package OPAC, Bulletin of the A merican Met. Soc. **79**, 5, p831-844.

[15] Chylek, P., and J. Wong (1995), Effect of absorbing aerosols on global radiation bud get, Geophys . Res. Lett. , 22(8), 929 – 931, doi: 10.1 029/95GL00800.

[16] Penner, J. E., Dickinson, R. E. and O'Neil, C. A. (1992). Effects of aerosol from biomass burning on the global radiation budget. Science, 256, 1432-1434.

[17] Segan, C. and Pollack, J. (1967). Anisotropic nonconservative scattering and the clouds of Venus. J. Geophys. Res. 72, 469-477.

[18] Aspens, D. E. (1982). Local-field effects and effective medium theory: A microscopic perspective. Am. J. Phys. 50, 704-709.

[19] Lorenz, L. (1880). Ueber die Refractionconstante. A nn. P hys. Chem. 11, 70–103.

[20] Lorentz, H. A. (1880). Ueber die Beziehung zwischen der Fortpflanzungsgeschwindigkeit des Lichtes und der Korperdichte. Ann. P hys. Chem. 9, 641–665.

[21] Ångström, A.K. (1961). Techniques of Determining the Turbidity of the Atmosphere. Tellus XIII: 214.

[22] Ångström, A., (1929). On the atmospheric transmission of sun radiation and on dust in the air. Geogr. Ann., 11, 156-166.

[23] Liu P. F., Zhao C. S., Gobel T., Hallbauer E., Nowak A., Ran L., Xu W. Y., Deng Z. Z., Ma N., Mildenberger K., Henning S., Stratmann F., and Wiedensohler A. (2011) Hygroscopic properties of aerosol particles at high relative humidity and their diurnal variations in the North China Plain, Atmos. Chem. Phys. Discuss., 11, 2991–3040

[24] O'Neill, N.T., T.F. Eck, B.N. Holben, A. Smirnov, O. Dubovik, and A. Royer, Uni and bi-modal size distribution influences on the variation of Angstrom derivatives in spectral and optical depth space, *J.Geophys.Res.,* 2000

[25] Dubovik, O., et. al., (2000): *Accuracy assessments of aerosol optical properties retrieved from Aerosol Robotic Network (AERONET) Sun and sky radiance measurments,* JGR, 105, 9791 - 9806.

[26] Eck, T. F., et al. (2005), Columnar aerosol optical properties at AERONET sites in central eastern Asia and aerosol transport to the tropical mid-Pacific, J. Geophys. Res. , 110 , D06202, doi:10.1029/2004JD005274

[27] Ranjan, R.R., Joshi, H.P. and Iyer, K.N. (2007). Spectral variation of total column aerosol optical depth over Rajkot: A tropical semi-arid Indian station. Aerosol Air Qual. Res. 7: 33-45.

[28] Kusmierczyk-Michulec J. and A.M.J. van Eijk, (2007), Ångström coefficient as a tracer of the continental aerosols, Proceedings SPIE vol. 6708-25, Atmospheric Optics: Models, Measurements, and Target-in the-Loop Propagation, 27-28 August 2007, San Diego, CA, USA.

[29] Swietlicki, E.,et. al. (2008) Hygroscopic properties of submicrometer atmospheric aerosol particles mea-sured with H TDMA instruments in various environments – A review, Tellus B, 60, 432–469,.

[30] Randles , C. A. , Russell L. M. and. Ramaswamy V. (2004) Hygroscopic and optical properties of organic sea salt aerosol and consequences for climate forcing, Geophysical Research Letters, Vol. 31, L16108, doi:10.1029/2004GL020628.

[31] Penner, J.E., et al., (1994). Quantifying and minimizing uncertainty of climate forcing by anthropogenic aerosols. Bulletin of the American Meteorological Society 75, 375–400.

[32] IPCC (2001): Climate Change 2001: The Scientific Basis. Houghton et al., Eds., Cambridge University Press, New York. 896 pp.

[33] Carrico, C.M., Kus, P., Rood, M.J., Quinn, P.K., Bates, T.S., (2003). Mixtures of pollution, dust, sea salt, and volcanic aerosol during ACE-Asia: radiative properties as a function of relative humidity. Journal of Geophysical Research 108 (D23), 8650.

[34] Doherty, et al., 2005. A comparison and summary of aerosol optical properties as observed in situ from aircraft, ship, and land during ACE-Asia. Journal of Geophysical Research 110, D04201.

[35] Quinn, P. K., et al. (2005) , Impact of particulate organic matter on the relative humidity dependence of light scattering: A simplified parameterization, Geophys. Res. Lett., 32, L22809, doi:10.1029/2005GL024322.

[36] Gasso S., et al. (2000), Influence of humidity on the aerosol scattering coefficient and its effect on the upwelling radiance during ACE-2, Tellus, Ser. B , 52, 546 – 567.

[37] Clarke, A., et al. (2007), Biomass burning and pollution aerosol over North America: Organic components an d their influence on spectral optical properties and humidification response, J. Geophys. Res., 11 2, D12S18, doi:10.1029/2006JD007777.

[38] Dubovik, O., Holben, B. N., Eck, T. F., Smirnov, A., Kaufman, Y. J., King, M. D., Tanre, D., and Slutsker, I.(2002): Climatology of atmospheric aerosol absorption and optical properties in key locations, J. Atmos. Sci., 59, 590–608.

[39] Schuster, G.L., Dubovik, O. and Holben, B.N. (2006). Angstrom Exponent and Bimodla Aerosol Size Distributions. J. Geophy. Res. 111: 7207.

[40] Fitzgerald, J. W. (1975) Approximation formulas for the equilibrium size of an aerosol particle as a function of its dry size and composition and ambient relative humidity. J. Appl. Meteorol., 14, 1044 –1049

[41] Tang, I. N. (1996) Chemical and size effects of hygroscopic aerosols on light scattering coeffcients. J. Geophys . R es. , 101, 19245 – 19250.

[42] Anderson, T. L. and Ogren, J. A.:(1998) Determining aerosol radiative properties using the TSI 3563 integrating nephelometer, Aerosol. Sci. Tech., 29, 57–69,.

[43] Xu, J., Bergin, M. H., Yu, X., Liu, G., Zhao, J., Carrico, C. M., and Baumann, K.:(2002) Measurement of aerosol chemical, physical and radiative properties in the Yangtze delta region of China, Atmos. Environ., 36, 161–173,.

[44] Reid, J. S. et al., (1998), Physical, Chemical and optical of regional hazes dominated by smoke in Brazil, J. Geophys. Res. 103, 32,059-32,080.

[45] Carrico, C.M., Rood, M.J., Ogren, J.A.(1998) Aerosol light scattering properties at Cape Grim, Tasmania, during the First Aerosol Characterization Experiment (ACE 1), J. Geophys. Res ., 103, 16565-16574.

[46] Bergstrom, R. W., Russell, P. B., and Hignett, P. B.(2002): The wavelength dependence of black carbon particles: predictions and results from the TARFOX experiment and implications for 20 the aerosol single scattering albedo, J. Atmos. Sci., 59, 567–577.

[47] Noh Y. M. et. al., (2009) Optical and microphysical properties of severe haze and smoke aerosol measured by integrated remote sensing techniquies in Gwangju, Korea, Atmos. Env. 43, 879 - 888

[48] Ansmann, A., Engelmann R., Althausen D.,Wandinger U., Hu, M. M, Zhang, Y.,(2005). High aerosol load over Pearl River Delta, China, observed with Raman lidar and Sun photometer. Geophysical Research Letters 32, L13815.

[49] Cattrall, C., Reagan, J., Thome, K., Dubovik, O.,(2005). Variability of aerosol and spectral lidar and backscatter and extinction ratios key aerosol types derived from selected Aerosol Robotic Network locations. Journal of Geophysical Research 110, D10S11. doi:10.1029/2004JD005124.